SPERM ULTRASTRUCTURE OF THE SPIDER CRAB *Maja brachydactyla* (Decapoda: Brachyura).

Authors' names

Carles G. Simeó[1]*, Kathryn Kurtz[2], Guiomar Rotllant[1], Manel Chiva[2], Enric Ribes[3]*

Institutions

1 IRTA Sant Carles de la Ràpita

2 Departament de Ciències Fisiològiques II, Universitat de Barcelona

3 Departament de Biologia Cel·lular, Universitat de Barcelona

Short title:

Sperm of *Maja brachydactyla*

*** Corresponding authors**:

Carles G. Simeó, IRTA Sant Carles de la Ràpita, Ctra. del PobleNou km 5.5, 43540 Sant Carles de la Ràpita, Spain. E-mail: carlos.garcia@irta.cat. Phone number: 0034 977 547 427, fax number: 0034 977 544 138.

Enric Ribes, Departament de Biologia Cel·lular, Universitat de Barcelona. Av Diagonal, 645, 08028 Barcelona, Spain. E-mail: eribes@ub.edu.

ABSTRACT

This work describes the morphology of the sperm cell of *Maja brachydactyla*, with emphasis on localizing actin and tubulin. The spermatozoon of *M. brachydactyla* is similar in appearance and organization to other brachyuran spermatozoa. The spermatozoon is a globular cell composed of a central acrosome, which is surrounded by a thin layer of cytoplasm, and a cup-shaped nucleus with four radiating lateral arms. The acrosome is a subspheroidal vesicle composed of three concentric zones surrounded by a capsule. The acrosome is apically covered by an operculum. The perforatorium penetrates the center of the acrosome and has granular material partially composed of actin. The cytoplasm contains one centriole in the subacrosomal region. A cytoplasmic ring encircles the acrosome in the subapical region of the cell and contains the structures-organelles complex (SO-complex), which is composed of a membrane system, mitochondria with few cristae, and microtubules. In the nucleus, slightly condensed chromatin extends along the lateral arms, in which no microtubules have been observed. Chromatin fibers aggregate in certain areas and are often associated to the SO-complex. During the acrosomal reaction, the acrosome could provide support for the penetration of the sperm nucleus, the SO-complex could serve as an anchor point for chromatin, and the lateral arms could play an important role triggering the acrosomal reaction, while slightly decondensed chromatin may be necessary for the deformation of the nucleus.

Key words:

Maja brachydactyla, spermatozoa, morphology, acrosome, microtubules, chromatin

INTRODUCTION

The spermatozoon of Brachyura is generally described as a non-flagellated cell with a globular acrosome, often surrounded by a fine layer of cytoplasm, and a nucleus located in the periphery that extends into several radiating arms (Jamieson and Tudge, 2000). Numerous ultrastructural variations have been described and used as characteristics to validate morphological and molecular-based phylogenetic studies (Jamieson, 1994). For example, the separation between the Gecarcinucidae and Potamidae families in the Potamoidea is confirmed by the presence of a middle acrosomal layer in the sperm of the Potamidae (represented by the subfamily Potamiscinae in Klaus et al., 2009). Similarly, the differences observed between the spermatozoa of *Macropodia longirostris* (Jamieson et al., 1998) and *Inachus phalangium* (Rorandelli et al., 2008) and the rest of Majoidea, including the spider crab *Maja brachydactyla*, support the existence of a taxonomic unit within the Inachinae, as suggested by larval studies (see discussion in Rorandelli et al., 2008).

Aside from its phylogenetic importance, the study of the morphology and composition of brachyuran spermatozoa can contribute to our understanding of the complex mechanisms of gamete fertilization in these animals. Several authors have described that during the first phases of gamete contact, the acrosome undergoes an eversion (Fasten, 1921; Hinsch, 1971; Goudeau, 1982; Nanshan and Luzheng, 1987; Krol et al., 1992; Medina and Rodríguez, 1992a), initiating the motion of the sperm nucleus toward the oocyte. In some studies, the presence of actin in the perforatorium suggests that polymerization of actin could have an active role in the acrosomal eversion (Hernandez et al., 1989). In addition, actin has been found in the lateral arms of the nucleus, and myosin occupies the basal portion of the lateral arms (Perez et al., 1986; Hernandez et al., 1989).

The consistency and composition of the nucleus are also important characteristics. Chromatin in the sperm nucleus of most brachyurans appears decondensed and fluid-like (Brown, 1966; Langreth 1969; Hinsch 1969, 1986; Medina and Rodríguez, 1992b). These properties are necessary in nuclei that must undergo mechanic deformation in order to enter the oocyte (Talbot and Chanmanon, 1980; Goudeau, 1982). Despite its malleability, the chromatin must also possess a minimum consistency in order to penetrate the oocyte without causing DNA breakage. In this regard, the chromatin close to the acrosome in *I. phalangium* is more electron-dense (greater condensation according to Rorandelli et al. 2008) than the chromatin located in the nuclear periphery. In this case, the dense inner chromatin could better resist the mechanical traction exerted during the acrosomal eversion.

Here, we complement the study of spermiogenesis of *Maja brachydactyla* (Simeó et al., 2009) by describing the morphology of the spermatozoon of this species and the distribution of actin and tubulin.

MATERIALS AND METHODS

Animals

Mature male specimens of *Maja brachydactyla* Balss, 1922 were captured in Galicia, Northwest Spain, by artisanal coastal fishery using gillnets between November 2006 and July 2007. Each animal was anesthetized on ice for at least 10 minutes, until they did not respond to external stimuli, heart was dissected causing the death of the animal and testis and vas deferens were then removed. The experimental procedure conforms to the current animal protection regulations (86/609/CEE, RD 1201/2005, and D 214/1997).

Transmission electron microscopy (TEM)

Small pieces of testes and vas deferens were fixed in a mixture of 2% paraformaldehyde and 2.5% glutaraldehyde in cacodylate buffer (0.1 mol L^{-1}, pH 7.4) for 24 h at 4ºC. Samples were rinsed in cacodylate buffer (3 times for 10 minutes and 3 times for 30 minutes) and post-fixed for 1 hour and 30 minutes at 4ºC in 1% osmium tetroxide in cacodylate buffer. The samples were then rinsed in cacodylate buffer twice for 5 minutes and once for 30 minutes. Fixed tissue samples were dehydrated through graded series of acetone and embedded in Spurr's resin. Ultrathin sections were made using a Leica UCT ultramicrotome and counterstained with uranyl acetate and lead citrate. Observations were made with a Jeol EM-1010 transmission electron microscope at 80 kV. Cellular measurements were made using an image analyzing system (AnalySIS, SIS).

Scanning electron microscopy (SEM)

Fresh testis and vas deferens tissue were dissected in PBS, and cell suspensions were placed on glass slides pre-treated with poly-L-lysine. Tissue samples were fixed in a mixture of 2% paraformaldehyde and 2.5% glutaraldehyde in cacodylate buffer (0.1 mol L^{-1}, pH 7.4) for 24 h at 4ºC. Samples were rinsed in cacodylate buffer (3 times for 10 minutes and 3 times for 30 minutes) and post-fixed for 1 hour and 30 minutes at 4ºC in 1% osmium tetraoxide in cacodylate buffer. Then, the samples were rinsed in cacodylate buffer twice for 5 minutes and once for 30 minutes. Progressive dehydration of fixed tissue samples was done in an ascending ethanol series. Following dehydration, samples were critical point dried and sputter coated with gold-palladium. Observations were made with a Hitachi S-2300 scanning electron microscope at 10-15 kV.

Confocal immunomicroscopy and epifluorescence microscopy

Confocal immunofluorescence was performed based on the technique used in Tudge et al. (1994) with some variations. Fresh testis and vas deferens tissue were dissected in PBS, and cell suspensions were placed on glass slides pretreated with poly-L-lysine, air-dried for 2 hours, and refrigerated overnight. The slides were then fixed in 3% paraformaldehyde, 60 mmol L^{-1} glucose in phosphate buffer (0.1 mol L^{-1}, pH 7.4) for 20 minutes at 4 ºC, washed three times in PBS for 15 minutes each, and blocked with PBS containing 1% BSA for 30 minutes using a humid chamber. The slides were then incubated overnight at 4°C in the humid chamber with anti-β-tubulin antibody (Amersham Biosciences, Munich, Germany) diluted 1:25 in the same solution used for blocking. Next day, samples were washed several times with PBS containing 0.1% Tween-20, followed by a wash with PBS. The samples were then incubated for 1 hour in a humid chamber with the secondary antibody Alexa Fluor 488 goat anti-rabbit IgG (Molecular probes, Camarillo, CA, USA) diluted 1:500 in PBS containing 0.1% Tween-20 and 1% BSA. After the secondary antibody incubation, the slides were treated for 20 minutes with rodaminated phalloidin (Sigma, St. Louis, MO, USA) to highlight actin, and for 5 minutes with 1% bisbenzimide (Hoechst 33258) in PBS to stain nuclear material. Finally, the slides were washed in PBS, mounted with Immunofluore mounting media (MP Biomedicals, Heidelberg, Germany), and dried overnight at 4°C before observation with a Leica DMRD confocal fluorescence microscope.

RESULTS

General description of the spermatozoa

Mature sperm cells are packed into spermatophores in the median vas deferens. The spermatophores of *M. brachydactyla* vary in size and contain between a few up to several

hundreds of sperm cells, which are separated by an intercellular matrix (Fig. 1A). The mature spermatozoon of *M. brachydactyla* is a star-shaped cell, with a globular body approximately 5 μm long and 7 μm wide and four radiating arms (Fig. 1B). The sperm cell is composed of a complex acrosome, a thin layer of cytoplasm, and a cup-shaped nucleus. The acrosome is the most voluminous structure of the spermatozoon and appears as an electron-dense body that fills the center of the sperm cell (Fig. 1A). The cytoplasm is located between the acrosome and the nucleus. The nucleus is positioned in the periphery of the cell and extends throughout the radiating lateral arms. Both, the acrosome, except in the apical region, and the cytoplasm are surrounded by the nucleus (Fig. 1B).

Acrosome

The acrosome is a subspheroidal, complex vesicle that measures around 4 μm in length and 5 μm in width. It consists of three concentric layers of different electron densities (external, intermediate, and internal acrosomal layers), a central perforatorium, and an operculum in the apical region (Fig. 2A). The internal acrosomal layer is the most electron-dense of the three concentric layers, and the intermediate layer is the least electron-dense (Fig. 2A,B). A capsule envelopes the external acrosomal layer (Fig. 3C). The capsule is a thin (35 ± 5 nm) lightly electron-dense layer limited by the acrosomal membrane, which is in close association with the nuclear envelope.

The operculum is the most electron-dense structure of the spermatozoon and is centrally depressed (Fig. 2 A). In fully mature spermatozoa, the operculum shows a small protuberance in its center (Fig. 4D).

The perforatorium is a central rhomboidal column that crosses the acrosome up to the operculum following the anterior-posterior axis of the cell (Fig. 2A). The basal region of the perforatorium

153 is separated from the cytoplasm by a discontinuous membrane (Fig. 3B). In this region the
154 thickened ring, an electron-dense band of the acrosome associated to the base of the
155 perforatorium, is also observed (Figs. 2A and 3B). The perforatorium contains granular material
156 in the upper half and small, granular, rod-shaped matter in the basal area (Figs. 2A,C and 3A,B).
157 A positive reaction with rodaminated phalloidin indicates that actin forms part of this material
158 (Fig. 5B).

159 **Cytoplasm**

160 The cytoplasm is a sparse, thin layer between the acrosome and the nucleus and is only
161 noticeable below the perforatorium and around the subapical region of the spermatozoon (Fig.
162 2A). Only in these regions, the cytoplasm contains the organelles (Fig. 3A). In the basal region
163 of the perforatorium, one centriole is found (Fig. 3A,B). In the subapical region of the
164 spermatozoon, the cytoplasm forms a cytoplasmic ring (Figs. 2C and 4D), which surrounds the
165 operculum and contains a circular aggregate of structures and organelles called the structures-
166 organelles complex (SO-complex) (Figs. 2A,B and 3A). The SO-complex is composed of a
167 membrane system that wraps around an accumulation of microtubules and some mitochondria
168 with few cristae (Fig. 3C-E). Both the centriole and the SO-complex intensely react with anti-β-
169 tubulin antibody (Fig. 5B).

170 **Nucleus**

171 The sperm nucleus of *M. brachydactyla* is a cup-shaped structure with four lateral arms that
172 surrounds the acrosome, with the exception of the operculum (Figs. 2A,C and 4C). The nucleus
173 contains decondensed chromatin that, here, is organized into fibers of 10 nm (Fig. 3E,F). The
174 chromatin fibers extend along the lateral arms (Fig. 3F), as confirmed by their reaction with
175 Hoechst fluorescent dye (Fig. 5B). Occasionally, the chromatin fibers are aggregated in electron-

dense areas throughout the nucleus, some of them appearing close to the SO-complex (Fig. 3D-F). The absence of reaction with either rodaminated phalloidin or anti-β-tubulin (Fig. 5B) indicates that no microtubules or any other cellular cytoskeleton components are found in the lateral arms.

The lateral arms develop during the last phases of spermiogenesis. While immature spermatozoa obtained from the transformation zone of the seminiferous tubule contain poorly developed or no lateral arms (Fig. 4A,B), the nucleus of the mature spermatozoa found in the evacuation zone already presents the four, well-developed lateral arms (Fig. 4C). Each lateral arm is approximately 9 μm long (Fig. 4C). Occasionally, the spermatozoa present only three lateral arms (Fig. 5A). In all spermatozoa observed, morphogenesis of the lateral arms, both in position and in length, is remarkably regular.

The nuclear envelope appears as a thick, electron-dense wall (Fig. 3F). However, it presents some discontinuities along the inner edge, where the nuclear envelope is in contact with the acrosome (white arrows in Fig. 3E).

DISCUSSION

Terminological considerations

The different structures of the spermatozoon have been termed according to the most accepted denominations in the literature (Table 1), with the exception of the structures-organelles complex. While the denominations acrosome, perforatorium, and operculum, including their derivatives, are widely accepted, the terminology of the complex composed of the membrane system, mitochondria, and occasionally the microtubules that encircle the acrosome is highly variable. We believe previous denominations of this complex are not appropriate because they place too much emphasis on the membrane system but mask the presence of mitochondria and

199 microtubules. Therefore, we propose the novel term structures-organelles complex (SO-
200 complex), in which structures refer to the membrane systems and microtubules, while organelles
201 refer to mitochondria. Although the role of the complex is not yet clear, bringing together the
202 different components of the complex under the generic term SO-complex reflects the close
203 relationship observed between the three components during spermiogenesis in *M. brachydactyla*
204 (Simeó et al., 2009). In addition, using a generic name may facilitate the morphological
205 descriptions of the brachyuran spermatozoa, addressing the differences of the development of the
206 components between species, as well as further comparisons for taxonomical studies. We are
207 aware that the denomination SO-complex is based on morphological observations, and a more
208 proper term could be found in the future, as more information about its development and
209 function becomes available.

210 **Sperm morphology of *M. brachydactyla***

211 The spermatozoon of *M. brachydactyla* exhibits the appearance and general organization of the
212 brachyuran spermatozoon (Jamieson, 1994). The sperm cell is non-flagellated and is composed
213 of a central spheroidal acrosome, surrounded by a thin layer of cytoplasm, and a cup-shaped
214 nucleus with four lateral arms. The spermatozoon shares most of the traits of the spermatozoa of
215 the Majoidea superfamily, such as the broad and centrally depressed operculum, the rhomboidal
216 and short perforatorium, the concentric zonation of the acrosome, and the presence of centrioles
217 (Jamieson et al., 1998; Jamieson and Tudge, 2000). Other characters observed in several
218 Majoidea are absent: the posterior median process (Hinsch, 1969, 1973), the presence of
219 microtubules in the lateral arms (Hinsch, 1969, 1973), and the perforation of the operculum
220 (Jamieson, 1991; 1994; Jamieson and Tudge, 2000). We summarize the presence, absence, and
221 the type of characters used by Jamieson (1994) for cladistic analysis in Table 2, while the

222 relative position and structural elements of the spermatozoon components of *M. brachydactyla*
223 are represented in Fig. 6.
224 The acrosome is the most prominent component of the spermatozoa in *M. brachydactyla* and
225 follows the general pattern observed in Majoidea (Hinsch, 1973; Chiba et al., 1992; Jamieson et
226 al., 1998). However, the subspheroidal shape of the acrosome contrasts with the strongly
227 depressed acrosome of *Macropodia longirostris* (Jamieson et al., 1998) and *Inachus phalangium*
228 (Rorandelli et al., 2008). The acrosome is organized into three concentric layers of different
229 electron densities, all surrounded by a capsule, covered apically by the operculum, and centrally
230 penetrated by the perforatorium. In addition, the thickened ring is also observed. While the three-
231 coat morphology and organization of the acrosome in *M. brachydactyla* is similar to that of other
232 Majoidea, such as *Libinia* sp. (Hinsch, 1969) and *Chionoecetes opilio* (Chiba et al., 1992), it
233 differs from the description of *M. brachydactyla* with only two separate layers given by Tudge
234 and Justine (1994). The internal acrosomal layer of *M. brachydactyla* spermatozoa may be
235 homologous to the inner acrosome zone described by Tudge and Justine (1994, as *Maja*
236 *squinado*); however, the homology is unclear for the outer acrosome zone of Tudge and Justine
237 (1994) and the external and intermediate acrosomal layers of *M. brachydactyla.*
238 The presence of actin in brachyuran spermatozoa has been reported in several species with a
239 variable distribution (Tudge et al., 1994; Rorandelli et al., 2008). Actin in *M. brachydactyla*, as
240 in *I. phalangium* (Rorandelli et al., 2008), is restricted to the basal region of the perforatorium,
241 while in *Cancer pagurus* (Tudge et al., 1994), actin is present in the perforatorium as well as in
242 two concentric rings of the acrosome.
243 The highly reduced cytoplasm of *M. brachydactyla* sperm cells is more apparent in the base of
244 the perforatorium and in the cytoplasmic ring, contrary to the conspicuous cytoplasm observed in

the spermatozoa of *Jasus novaehollandiae* (Tudge et al., 1998) and *Pylocheles* sp. (Tudge et al., 2001). The base of the perforatorium contains at least one centriole, as described in *C. opilio* (Chiba et al., 1992), but we do not discard the presence of two centrioles as in other Majoidea (Jamieson et al., 1998). The cytoplasmic ring is filled with the structures-organelles complex (SO-complex), which is composed of a membrane system, microtubules, and very simplified mitochondria with few cristae. The SO-complex of *Carcinus maenas* (Pochon-Masson, 1968), *Cancer* sp. (Langreth, 1969), and *Neodorippe astuta* (Jamieson and Tudge, 1990) has the same components (membranes, mitochondria, and microtubules) as *M. brachydactyla*, while the SO-complex in most brachyuran species only contains membranes and mitochondria (see SO-complex section in Table 1 for references).

The sperm nucleus of *M. brachydactyla* presents an electron-dense complex envelope, derived from the fusion of the outer edge of the plasma membrane and the nuclear envelope during spermiogenesis (Simeó et al., 2009), similar to other brachyurans (Hinsch, 1988; Chiba et al., 1992). The nucleus of the sperm cell generally has four radial arms, occasionally only three situated laterally. The number of nuclear arms varies among Majoidea, showing three in some species (Hinsch, 1969; Jamieson et al., 1998), between 4 and 10 in *C. opilio* (Chiba et al., 1992), and 5 radial arms with several ventral protrusions in *I. phalangium* (Rorandelli et al., 2008). While the lateral arms of *L. emarginata* (Hinsch, 1969) contain chromatin and microtubules, the lateral arms of *M. brachydactyla* only seem to contain chromatin; neither microtubules nor β-tubulin were observed using TEM or immunofluorescence microscopy. We did not observe the source for the development of the lateral arms, neither during spermiogenesis (Simeó et al., 2009), nor in mature spermatozoa.

Chevaillier (1970) and Reger et al. (1984) demonstrated in some decapods that the morphology of the nucleus depends on the method of fixation applied. Nevertheless, our methods seem to obtain reproducible results, which we describe and discuss below. The chromatin is non-condensed and is organized into fibers of approximately 10 nm of diameter, similar to the size of a nucleosome (see the discussions of Kurtz et al., 2007; Martínez-Soler et al., 2007b). Indeed, the chromatin does not seem to be organized into superior structures like the granules or fibers with a diameter of 20 nm or greater observed in other non-crustacean species (Gimenez-Bonafé et al., 2002; Martínez-Soler et al., 2007a; Kurtz et al., 2009b). However, the chromatin is not completely uniform throughout the nucleus, and the chromatin fibers appear to agglutinate in several more electron-dense areas, around the SO-complex and at the base of the lateral arms. We do not reject the possibility that part of the chromatin could be bound to the SO-complex through the nuclear envelope, similar to the anchorage of chromatin to the nuclear envelope, covered by microtubules, observed in other spermiogenesis (Kessel and Spaziani, 1969; Soley, 1997; Martínez-Soler et al., 2007a).

Despite the possible relation between the nuclear lateral arms and the chromatin aggregates, the causes and mechanical elements that determine the development of the four nuclear arms remain unknown. In this regard, the presence and role of the sperm nuclear matrix in the organization of the nucleus in the brachyuran spermatozoon, which has been described in the sperm of mammals (e.g., Ward and Coffey, 1990; Nadel et al., 1995; Kramer and Krawetz, 1996), should be investigated in further studies.

Origin and function of some sperm organelles

The acrosome, including the perforatorium, is the most complex organelle in the non-flagellated sperm of brachyurans and provides the necessary movements for the sperm nucleus to penetrate

290 the oocyte envelope and reach the oocyte cytoplasm (Brown, 1966; Hinsch, 1971; Goudeau,
291 1982; Medina and Rodríguez, 1992a). In *M. brachydactyla*, the acrosomal layers form
292 independently of each other during spermiogenesis (Simeó et al., 2009), and the internal
293 acrosomal layer and the perforatorium appear to have a coordinated self-organization in the later
294 phases of spermiogenesis. The internal acrosomal layer originates from an electron-dense vesicle
295 formed in the cytoplasm that later merges with the proacrosomal vesicle. Then, the perforatorium
296 develops from an invagination of the proacrosomal vesicle simultaneously with the elongation of
297 the electron-dense granule, which constitutes the internal acrosomal layer. These facts suggest
298 that the composition and function of the acrosomal layers could be complementary during the
299 acrosomal eversion.
300 The SO-complex is composed of a membrane system, which is derived from the degeneration of
301 the endoplasmic reticulum and Golgi complex, along with mitochondria with poorly developed
302 cristae, and microtubules (Simeó et al., 2009). Among other functions, the SO-complex could
303 serve as an anchor point for the chromatin and provide the necessary mechanic stability to push
304 the chromatin (by way of frontal traction) toward the oocyte during the acrosomal eversion (see
305 descriptions of the acrosomal eversion in Brown, 1966; Hinsch, 1971; Goudeau, 1982; Medina
306 and Rodríguez, 1992a). The different degrees of chromatin condensation observed in the sperm
307 of the Majoidea *I. phalangium* (Rorandelli et al., 2008) could be related to the nuclear traction
308 described during the first stages of fertilization.
309 In brachyuran spermatozoa, the lateral arms could be involved in triggering the acrosomal
310 reaction. Attachment of the spermatozoa to the oocytes occurs through the operculum and lateral
311 arms, and is followed by the acrosomal reaction (Brown, 1966; Hinsch, 1971; Medina, 1992).
312 The lateral arms increase the contact surface between gametes, which may be necessary to

313 provoke an ion transport that triggers the acrosomal reaction, as suggested by experimental
314 activation of the acrosomal reaction using calcium ionophore treatments or rich-calcium
315 solutions (Fasten, 1921; Nanshan and Luzheng, 1987; Medina and Rodríguez, 1992a).
316 Finally, poor condensation of the sperm chromatin is most likely indispensable to this type of
317 gamete fertilization. The chromatin in the mature sperm of most non-crustacean species is highly
318 compact due to the presence of highly basic DNA-interacting proteins, such as histones (without
319 any post-translational modifications) or other proteins (SNBPs, protamines) with a high content
320 of arginine or lysine residues (reviewed in Kasinsky, 1989). However, the DNA in the sperm
321 nucleus of *C. pagurus* (Kurtz et al., 2008) and *M. brachydactyla* (Kurtz et al., 2009a) is bound to
322 hyperacetylated histones (histone H4 in *C. pagurus* and histone H3 in *M. brachydactyla*).
323 Hyperacetylation prevents the condensation of chromatin into structures of higher order than
324 nucleosomes (Garcia-Ramirez et al., 1995; reviewed in Zheng and Hayes, 2003; Calestagne-
325 Morelli and Ausió, 2006), but it may also provide resistance to breakage as well as flexibility to
326 the nucleus during the acrosomal reaction.

327 **ACKNOWLEDGEMENTS**

328 The authors thank Núria Cortadellas and Almudena García (Serveis Científico-Tècnics de la
329 Universitat de Barcelona) and Josep Ma. Agulló (Centre de Recursos de la Universitat de
330 Barcelona) for their technical support. This study has been supported by the Spanish Ministry of
331 Environment and Rural and Marine Areas (JACUMAR), the Spanish Ministry of Education and
332 Science (BFU 2005-00123/BMC grant), the Catalonian Government (Xarxa de Referència de
333 Recerca, Desenvolupament i Innovació en Aquicultura, and the University and Research
334 Commission of the Innovation, University and Company Department) and the European Social
335 Fund.

336

LITERATURE CITED

Anilkumar G, Sudha K, Subramonian T. 1999. Spermatophore transfer and sperm structure in the brachyuran crab *Metopograpsus messor* (Decapoda: Grapsidae). J Crustacean Biol 19:361-370.

Benetti AS, Santos DC, Negreiros-Fransozo ML, Scelzo MA. 2008. Spermatozoal ultrastructure in three species of the genus *Uca* Leach, 1814 (Crustacea, Brachyura, Ocypodidae). Micron 39:337-343.

Brown GG. 1966. Ultrastructural studies of sperm morphology and sperm-egg interaction in the decapod *Callinectes sapidus*. J Ultra Res 14:425-440.

Calestagne-Morelli A, Ausió J. 2006. Long-range histone acetylation: biological significance, structural implications, and mechanisms. Biochem Cell Biol 84:518-527.

Chevaillier P. 1970. Recherches sur la structure et les constituants chimiques des cellules germinales mâles des crustacés décapodes [PhD thesis]. Rennes: Université de Rennes. 322 p.

Chiba A, Kon T, Honma Y. 1992. Ultrastructure of the spermatozoa and spermatophores of the zuwai crab, *Chionoecetes opilio* (Majidae, Brachyura). Acta Zool 73:103-108.

Cuartas EI, Sousa LG. 2007. Ultrastructure study of the spermatophores and spermatozoa in *Uca uruguayensis* (Decapoda, Brachyura, Ocypodidae). Biociências 15:21-28.

Du N, Xue L, Lai W. 1988. Studies on the sperm of Chinese mitten-handed crab, *Eriocheir sinensis* (Crustacea, Decapoda). 2. Spermatogenesis. Oceanol Limnol Sinica 19:71-75.

El-Sherief SS. 1991. Fine structure of the sperm and spermatophores of *Portunus pelagicus* (L.) (Decapoda, Brachyura). Crustaceana 61:271-279.

359 Fasten N. 1921. The explosion of the spermatozoa of the crab *Lophopanopeus bellus* (Stimpson)
360 Rathbun. Biol Bull 41:288-301.
361 Garcia-Ramirez M, Rocchini C, Ausió J. 1995. Modulation of chromatin folding by histone
362 acetylation. J Biol Chem 270:17923-17928.
363 Gimenez-Bonafé P, Ribes E, Sautière P, Gonzalez A, Kasinsky H, Kouach M, Sautière P-E,
364 Ausió J, Chiva M. 2002. Chromatin condensation, cysteine-rich protamine, and
365 establishment of disulphide interprotamine bonds during spermiogenesis of *Eledone*
366 *cirrhosa* (Cephalopoda). Eur J Cell Biol 81:341-349.
367 Goudeau M. 1982. Fertilization in a crab .1. Early events in the ovary, and cytological aspects of
368 the acrosome reaction and gamete contacts. Tissue Cell 14:97-111.
369 Hernandez W, Berry D, Baccetti B, Ahluwalia B, Murray SA, Anderson WA. 1989. Remodeling
370 of the nucleocytoplasm as consequence of the acrosomal reaction of the spider crab
371 sperm. J Submicrosc Cytol Pathol 21:163-186.
372 Hinsch GW. 1969. Microtubules in the sperm of the spider crab, *Libinia emarginata* L. J Ultra
373 Res 29:525-534.
374 Hinsch GW. 1971. Penetration of the oocyte envelope by spermatozoa in the spider crab. J Ultra
375 Res 35:86-97.
376 Hinsch GW. 1973. Sperm structure of Oxyrhyncha. Can J Zool 51:421-426.
377 Hinsch GW. 1986. A comparison of sperm morphologies, transfer and sperm mass storage
378 between two species of crab, *Ovalipes ocellatus* and *Libinia emarginata*. Int J Invertebr
379 Repr Dev 10:79-87.

Hinsch GW. 1988. Ultrastructure of the sperm and spermatophores of the golden crab *Geryon fenneri* and a closely related species, the red crab *G. quinquedens*, from the eastern gulf of Mexico. J Crustacean Biol 8:340-345.

Jamieson BGM. 1989. Ultrastructural comparison of the spermatozoa of *Ranina ranina* (Oxystomata) and of other crabs exemplified by *Portunus pelagicus* (Brachygnatha) (Crustacea, Brachyura). Zoomorphology 109:103-111.

Jamieson BGM. 1990. The ultrastructure of the spermatozoa of *Petalomera lateralis* (Gray) (Crustacea, Brachyura, Dromiacea) and its phylogenetic significance. Invertebr Reprod Dev 17:39-45.

Jamieson BGM. 1991. UItrastructure and phylogeny of crustacean spermatozoa. Mem Queensl Mus 31:109-142.

Jamieson BGM. 1994. Phylogeny of the Brachyura with particular reference to the Podotremata: Evidence from a review of spermatozoal ultrastructure (Crustacea, Decapoda). Philos Trans R Soc Lond B Biol Sci 345:373-393.

Jamieson BGM, Tudge CC. 1990. Dorippids are Heterotremata: evidence from ultrastructure of the spermatozoa of *Neodorippe astuta* (Dorippidae) and *Portunus pelagicus* (Portunidae) Brachyura: Decapoda. Mar Biol 106:347-354.

Jamieson BGM, Tudge CC. 2000. Progress in male gamete ultrastructure and phylogeny. In: Adiyodi KG, Adiyodi RG, editors. Reproductive Biology of Invertebrates. Kerala: John Wiley and Sons. p 1-95.

Jamieson BGM, Guinot D, Richer de Forges B. 1994. Podotreme affinities of *Raninoides* sp. and *Lyreidus brevifrons*: evidence from spermatozoal ultrastructure (Crustacea: Brachyura: Raninoidea). Mar Biol 120:239-249.

403 Jamieson BGM, Scheltinga DM, Richer de Forges B. 1998. An ultrastructural study of
404 spermatozoa of the Majidae with particular reference to the aberrant spermatozoon of
405 *Macropodia longirostris* (Crustacea, Decapoda, Brachyura). Acta Zool 79:193-206.
406 Jamieson BGM, Guinot D, Tudge CC, Richer de Forges B. 1997. Ultrastructure of the
407 spermatozoa of *Corystes cassivelaunus* (Corystidae), *Platepistoma nanum* (Cancridae)
408 and *Cancer pagurus* (Cancridae) supports recognition of the Corystoidea (Crustacea,
409 Brachyura, Heterotremata). Helgol Meeresunters 51:83-93.
410 Kasinsky H. 1989. Specificity and distribution of sperm basic proteins. In: Hnilica L, Stein G,
411 Stein J, editors. Histones and other basic nuclear proteins. Boca Raton, Florida: CRC
412 Press. p 73-163.
413 Kessel R, Spaziani E. 1969. Nuclear morphogenesis in rat spermatids. J Cell Biol 160:67a.
414 Klaus S, Schubart CD, Brandis D. 2009. Ultrastructure of spermatozoa and spermatophores of
415 Old World freshwater crabs (Brachyura: Potamoidea: Gecarcinucidae, Potamidae, and
416 Potamonautidae). J Morphol 270:175-193.
417 Kramer JA, Krawetz SA. 1996. Nuclear matrix interactions within the sperm genome. J Biol
418 Chem 271:11619-11622.
419 Krol RM, Hawkins WE, Overstreet RM. 1992. Reproductive components. In: Harrison FW,
420 Humes AG, editors. Microscopic Anatomy of Invertebrates. New York: Wiley-Liss, Inc.
421 p 295-343.
422 Kurtz K, Ausió J, Chiva M. 2009a. Preliminary study of sperm chromatin characteristics of the
423 brachyuran crab *Maja brachydactyla*. Histones and nucleosome-like structures in
424 decapod crustacean sperm nuclei previously described without SNBPs. Tissue Cell
425 doi:10.1016/j.tice.2009.02.003.

426 Kurtz K, Martínez-Soler F, Ausió J, Chiva M. 2007. Acetylation of histone H4 in complex
427 structural transitions of spermiogenic chromatin. J Cell Biochem 102:1432-1441.
428 Kurtz K, Martínez-Soler F, Ausió J, Chiva M. 2008. Histones and nucleosomes in *Cancer* sperm
429 (Decapod: Crustacea) previously described as lacking basic DNA-associated proteins: A
430 new model of sperm chromatin. J Cell Biochem 105:574-584.
431 Kurtz K, Saperas N, Ausió J, Chiva M. 2009b. Spermiogenic nuclear protein transitions and
432 chromatin condensation. Proposal for an ancestral model of nuclear spermiogenesis. J
433 Exp Zoolog B Mol Dev Evol 312B:149-163.
434 Langreth SG. 1969. Spermiogenesis in cancer crabs. J Cell Biol 43:575-603.
435 Li TW. 1995. On spermatogenesis and sperm ultrastructure of blue crab *Portunus trituberculatus*
436 (Crustacea, Decapoda). Acta Zool Sinica 41:41-47.
437 Martínez-Soler F, Kurtz K, Chiva M. 2007a. Sperm nucleomorphogenesis in the cephalopod
438 *Sepia officinalis*. Tissue Cell 39:99-108.
439 Martínez-Soler F, Kurtz K, Ausió J, Chiva M. 2007b. Transition of nuclear proteins and
440 chromatin structure in spermiogenesis of *Sepia officinalis*. Mol Reprod Dev 74:360-370.
441 Matos E, Matos P, Corral L, Azevedo C. 2000. Ultrastructure of spermatozoon of the crab
442 *Ucides cordatus* Linaeus (Crustacea, Decapoda) of the northern littoral of Brazil. Rev
443 Bras Zool 17:753-756.
444 Medina A. 1992. Structural modifications of sperm from the fiddler crab *Uca tangeri*
445 (Decapoda) during early stages of fertilization. J Crustacean Biol 12:610-614.
446 Medina A, Rodríguez A. 1992a. Structural changes in sperm from the fiddler crab, *Uca tangeri*
447 (Crustacea, Brachyura), during the acrosome reaction. Mol Reprod Dev 33:195-201.

448 Medina A, Rodríguez A. 1992b. Spermiogenesis and sperm structure in the crab *Uca tangeri*
449 (Crustacea, Brachyura), with special reference to the acrosome differentiation.
450 Zoomorphology 111:161-165.
451 Nadel B, de Lara J, Finkernagel S, Ward W. 1995. Cell-specific organization of the 5S ribosomal
452 RNA gene cluster DNA loop domains in spermatozoa and somatic cells. Biol Reprod
453 53:1222-1228.
454 Nanshan D, Luzheng X. 1987. Induction of acrosome reaction of spermatozoa in the decapoda
455 *Eriocheir sinensis*. Chin J Oceanol Limnol 5:118-123.
456 Perez RA, Langford GM, Eckberg WR, Anderson WA. 1986. Contractile proteins (actin,
457 myosin) and tubuline are revealed within DNA- containing nucleocytoplasm in mature
458 spermatozoa of *Libinia emarginata* L. J Submicrosc Cytol Pathol 18 471-480.
459 Pochon-Masson J. 1968. L'ultrastructure des spermatozoïdes vésicularies chez les crustacés
460 décapodes avant et au cours de leur dévegination expérimentale. I. Brachyoures et
461 Anomoures. Ann Sci Nat Zool 10:1-100.
462 Reger JF. 1970. Studies on the fine structure of spermatids and spermatozoa of the crab, *Pinnixia*
463 sp. J Morphol 132:89-100.
464 Reger JF, Escaig F, Pochon-Masson J, Fitzgerald MEC. 1984. Observations on crab, *Carcinus*
465 *maenas*, spermatozoa following rapid-freeze and conventional fixation techniques. J
466 Ultra Res 89:12-22.
467 Richer de Forges B, Jamieson BGM, Guinot D, Tudge CC. 1997. Ultrastructure of the
468 spermatozoa of Hymenosomatidae (Crustacea: Brachyura) and the relationships of the
469 family. Mar Biol 130:233-242.

Rorandelli R, Paoli F, Cannicci S, Mercati D, Giusti F. 2008. Characteristics and fate of the spermatozoa of *Inachus phalangium* (Decapoda, Majidae): Description of novel sperm structures and evidence for an additional mechanism of sperm competition in Brachyura. J Morphol 269:259-271.

Shang Guan B, Li SJ. 1994. On ultrastructure of the sperm of *Scylla serrata* (Crustacea, Decapoda, Brachyura). Acta Zool Sinica 40:7-11.

Simeó CG, Kurtz K, Chiva M, Ribes E, Rotllant G. 2009. Spermatogenesis of the spider crab, *Maja brachydactyla* (Decapoda: Brachyura). J Morphol.

Soley J. 1997. Nuclear morphogenesis and the role of the manchette during spermiogenesis in the ostrich (*Struthio camelus*). J Anat 190:563-576.

Talbot P, Chanmanon P. 1980. Morphological features of the acrosome reaction of lobster (*Homarus*) sperm and the role of the reaction in generating forward sperm movement. J Ultra Res 70:287-297.

Tudge CC, Justine JL. 1994. The cytoskeletal proteins actin and tubulin in the spermatozoa of 4 decapod crabs (Crustacea, Decapoda). Acta Zool 75:277-285.

Tudge CC, Grellier P, Justine JL. 1994. Actin in the acrosome of the spermatozoa of the crab, *Cancer pagurus* L (Decapoda, Crustacea). Mol Reprod Dev 38:178-186.

Tudge CC, Scheltinga DM, Jamieson BGM. 1998. Spermatozoal ultrastructure in the spiny lobster *Jasus novahollandiae* Holthuis, 1963 (Palinuridae, Palinura, Decapoda). J Morphol 236:117-126.

Tudge CC, Scheltinga DM, Jamieson BGM. 2001. Spermatozoal morphology in the "symmetrical" hermit crab, *Pylocheles (Bathycheles)* sp. (Crustacea, Decapoda, Anomura, Paguroidea, Pylochelidae). Zoosystema 23:117-130.

493 Wang L, Du N-S, Lai W. 1999. Studies on spermiogenesis of a freshwater crab *Sinopotamon*
494 *yangtsekiense* (Crustacea Decapoda). Acta Hydrobiol Sinica 23:29-33.
495 Wang YL, Zhang ZP, Li SJ. 1997. Ultrastructure of spermatogenesis in the crab *Scylla serrata*.
496 Acta Zool Sinica 43:249-254.
497 Ward WS, Coffey DS. 1990. Specific organization of genes in relation to the sperm nuclear
498 matrix. Biochem Biophys Res Commun 173:20-25.
499 Yasuzumi G. 1960. Spermatogenesis in animals as revealed by electron microscopy: VII.
500 Spermatid differentiation in the crab, *Eriocheir japonicus*. J Biophys Biochem Cytol
501 7:73-78.
502 Zheng C, Hayes JJ. 2003. Structures and interactions of the core histone tail domains.
503 Biopolymers 68:539-546.
504

505 FIGURE LEGENDS

506 Fig. 1. Partial view of a spermatophore located in the median vas deferens of *Maja*
507 *brachydactyla* containing ripe spermatozoa. (A) Transmission electron micrograph, (B)
508 scanning electron micrograph. A, acrosome; Arm, lateral or nuclear arms; N, nucleus.

509 Fig. 2. Transmission electron micrographs of the spermatozoa of *Maja brachydactyla* contained
510 within the spermatophore in the median vas deferens (A, B) and contained within the
511 evacuation zone of the seminiferous tubule in the testis (C). **A**. Radial section. **B**. Cross
512 section made approximately at the level indicated in A (see dashed line). **C**. Radial
513 section. A, acrosome; A1, external acrosomal layer; A2, intermediate acrosomal layer;
514 A3, internal acrosomal layer; Arm, lateral or nuclear arms; At, actin; Chr(+), more
515 densely arranged chromatin; CR, cytoplasmic ring; Cy, cytoplasm; N, nucleus; NE,
516 nuclear envelope; Op, operculum; P, perforatorium; SO, structures-organelles complex;
517 Tr, thickened ring.

518 Fig. 3. Transmission electron micrographs of the nucleus and cytoplasm of the spermatozoa of
519 *Maja brachydactyla*. **A**. Radial section of the spermatozoon, demonstrating the large size
520 and morphological complexity of the acrosome. **B**. Detail of the basal area of the
521 acrosome and the reduced area of cytoplasm where the centriole is found. **C**. Transversal
522 section of the structures-organelles complex composed of a series of membranes,
523 microtubules, and some mitochondria. **D**. Amplification of area D in image A showing
524 the membrane system that encircles the acrosome. **E**. The SO-complex of the cytoplasm,
525 showing its relation to the densely arranged chromatin fibers; also observe that the
526 nuclear envelope is discontinuous (white arrows). **F**. Detail of the nucleus located within
527 the lateral arms. The chromatin appears non-condensed and organized into fibers. A1,

external acrosomal layer; A2, intermediate acrosomal layer; A3, internal acrosomal layer; Arm, lateral or nuclear arms; At, actin; Ca, capsule; Ce, centriole; Chr, chromatin; Chr(+), more densely arranged chromatin; Chr(-), less densely arranged chromatin; Cy, cytoplasm; M, mitochondria; Ms, membrane system; Mt, microtubules; N, nucleus; NE, nuclear envelope; Op, operculum; P, perforatorium; SO, structures-organelles complex, Tr, thickened ring.

Fig. 4. Scanning electron micrographs documenting the development of the lateral arms at the end of the spermatogenesis in *Maja brachydactyla* observed in the seminiferous tubule of the testis. **A** and **B**. Spermatozoon released from the transformation zone. **C** and **D**. Mature spermatozoon obtained from the evacuation zone. Arm, lateral or nuclear arms; CR, cytoplasmic ring; N, nucleus; Op, operculum.

Fig. 5. Mature spermatozoon of *Maja brachydactyla*. **A**. Phase contrast microscopy. **B**. Confocal fluorescence microscopy. The reaction of the rodaminated phalloidin (red) in the center of the cell indicates the presence of actin in the perforatorium. The anti-β-tubulin antibody (green) binds to a ring that surrounds the acrosome and corresponds to the area occupied by the structures-organelles complex and the area where the centriole(s) is located (see also Fig. 3). The DNA is labeled by Hoechst intercalating dye (blue). A, acrosome; Arm, lateral or nuclear arms; Ce, putative centriole; N, nucleus; P, perforatorium; SO, structures-organelles complex.

Fig. 6. Schematic reconstruction of the mature spermatozoon of spider crab, *Maja brachydactyla*.

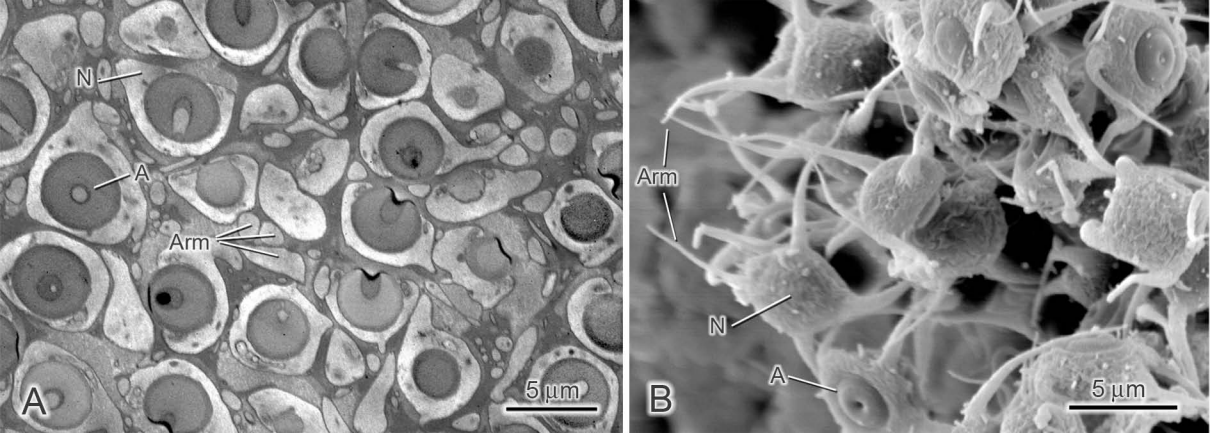
N
A
Arm
5 µm
A
Arm
N
A
5 µm
B

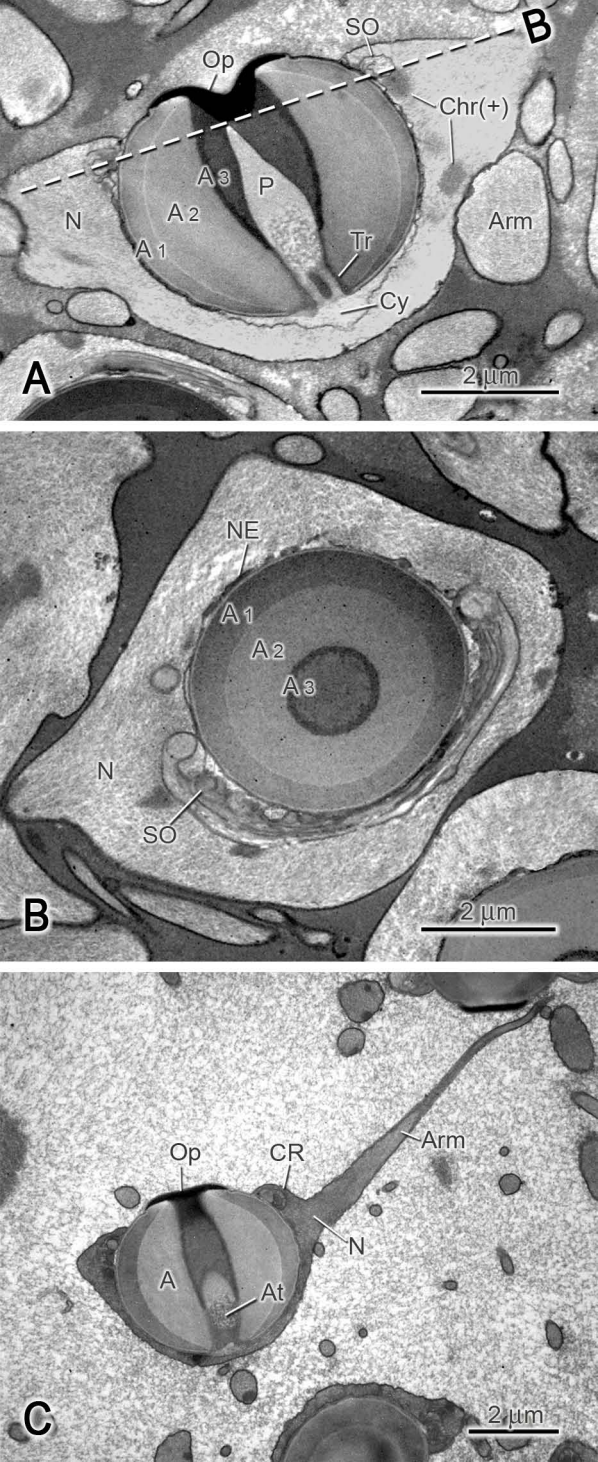
SO
B
Op
Chr(+)
A3
P
N
A2
Arm
A1
Tr
Cy
A
2 µm
NE
A1
A2
A3
N
SO
B
2 µm
Op
CR
Arm
N
A
At
C
2 µm

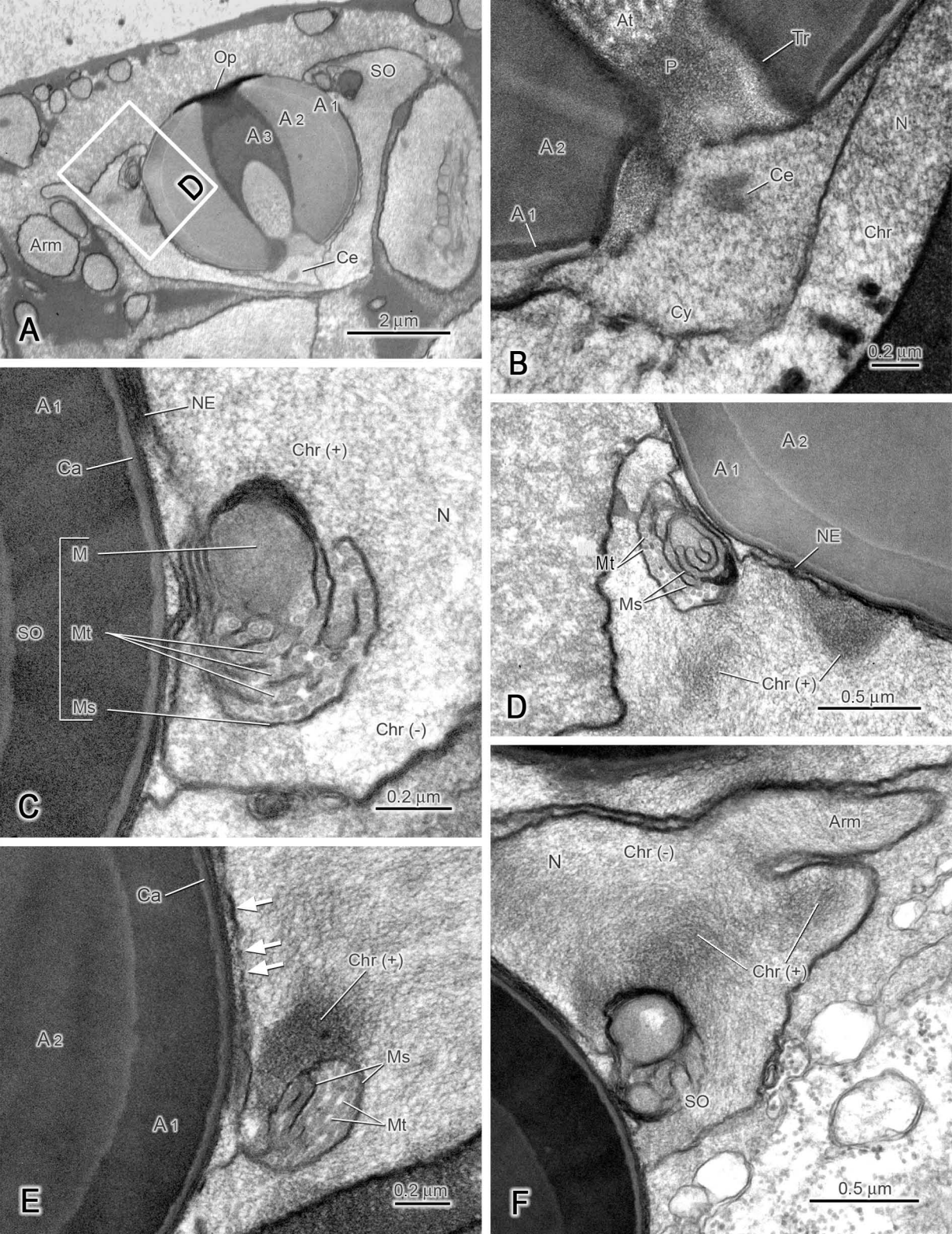
A
Op
SO
A 1
A 2
A 3
D
Arm
Ce
2 µm
B
At
Tr
P
N
A 2
Ce
A 1
Chr
Cy
0.2 µm
C
A 1
NE
Ca
Chr (+)
N
M
SO
Mt
Ms
Chr (-)
0.2 µm
D
A 2
A 1
NE
Mt
Ms
Chr (+)
0.5 µm
E
Ca
Chr (+)
A 2
Ms
A 1
Mt
0.2 µm
F
Arm
N
Chr (-)
Chr (+)
SO
0.5 µm

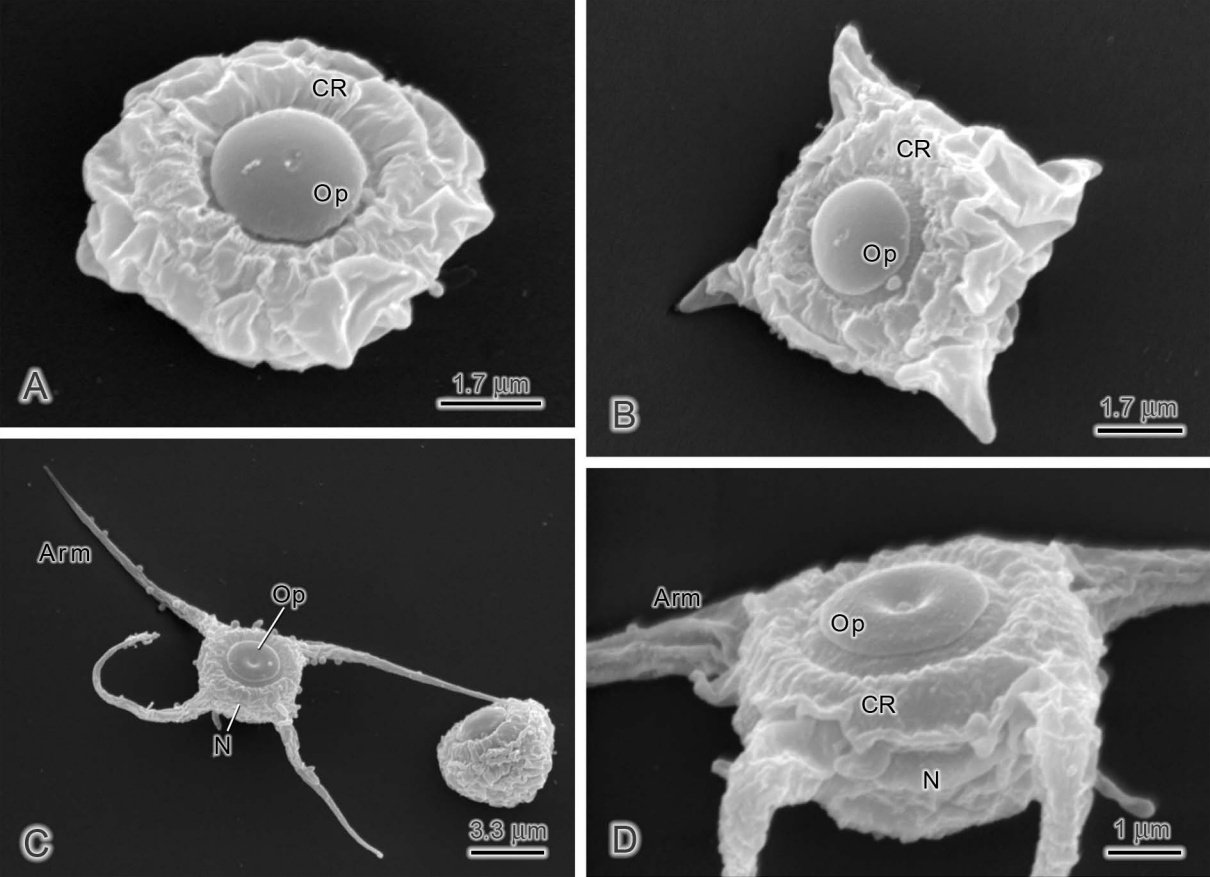
CR
Op
A
1.7 µm
CR
Op
B
1.7 µm
Arm
Op
N
C
3.3 µm
Arm
Op
CR
N
D
1 µm

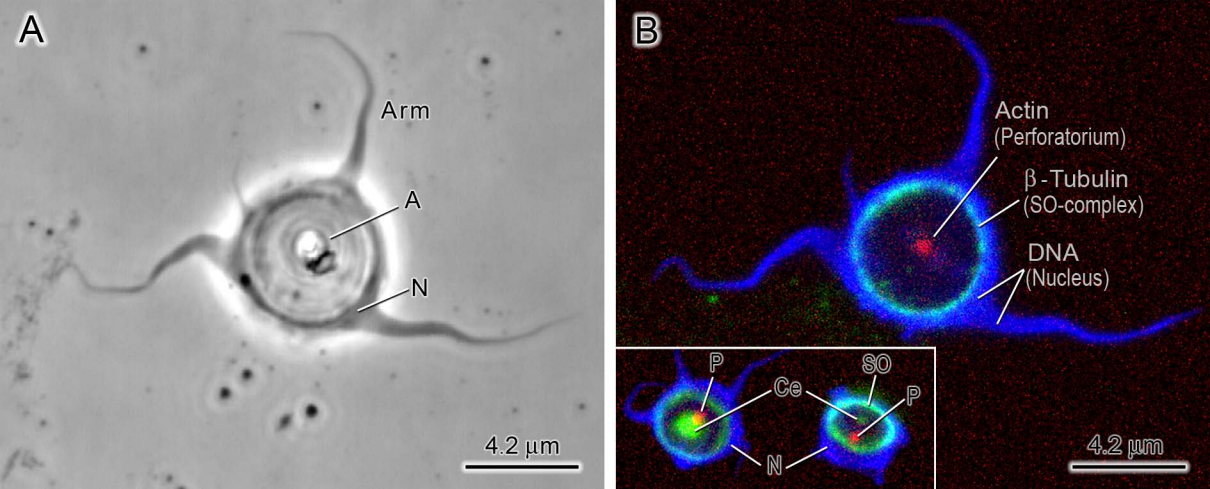
A
Arm
A
N
4.2 µm
B
Actin
(Perforatorium)
β-Tubulin
(SO-complex)
DNA
(Nucleus)
P
Ce
SO
P
N
4.2 µm

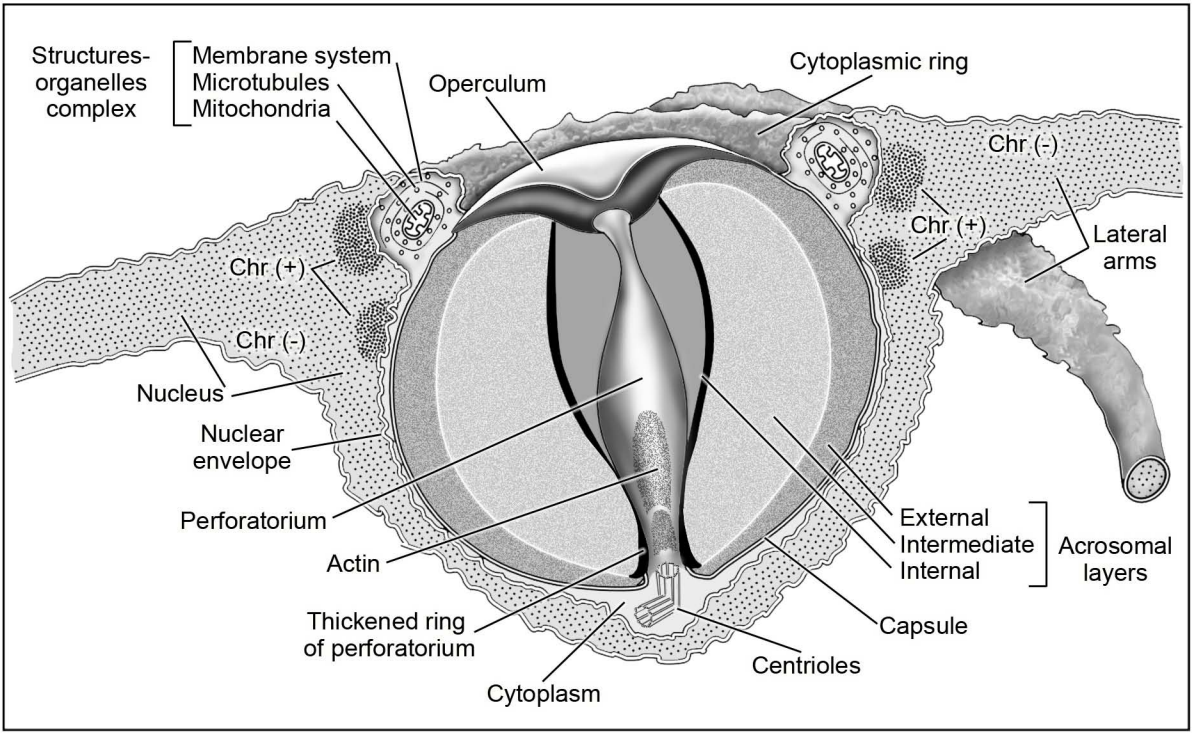
Structures-
organelles
complex
Membrane system
Microtubules
Mitochondria
Operculum
Cytoplasmic ring
Chr (-)
Chr (+)
Lateral
arms
Chr (+)
Chr (-)
Nucleus
Nuclear
envelope
Perforatorium
Actin
External
Intermediate
Internal
Acrosomal
layers
Capsule
Thickened ring
of perforatorium
Centrioles
Cytoplasm